J Mater Sci (2008) 43:1044–1049
DOI 10.1007/s10853-007-2262-x

Preparation and optoelectronic properties of *N*,*N*′-diphenyl-*N*,*N*′-bis(3-methylphenyl)-(1,1′-biphenyl)-4,4′-diamine/TiO_2 nanostructured hybrids

Yan-Gang Han · Gang Wu · Hong-Zheng Chen · Mang Wang

Received: 7 March 2007 / Accepted: 26 October 2007 / Published online: 15 November 2007

Abstract Organic–inorganic nanostructured hybrids based on *N*,*N*′-diphenyl-*N*,*N*′-bis(3-methylphenyl)-(1,1′-biphenyl)-4,4′-diamine (MTPD) and anatase TiO_2 were prepared via layer-by-layer deposition method. The MTPD/TiO_2 hybrids were characterized by UV–Vis absorption spectra, photoconductivity measurements, and surface photovoltage spectra (SPS). Due to the change of the aggregated structure caused by the addition of TiO_2, MTPD showed blue-shifted absorption spectrum. The photosensitivity of MTPD/TiO_2 nanostructured hybrids was increased by two times when compared with that of its single component. Studies on the SPS revealed that the efficient light-induced charge separation and transfer between MTPD and TiO_2 was responsible for the improved photosensitivity. The MTPD/TiO_2 hybrids exhibited high photosensitivity to ultraviolet light with weak intensity and acceptable stability under ultraviolet radiation, which endow the hybrids potential applications in the field of ultraviolet photodetection.

Y.-G. Han · G. Wu · H.-Z. Chen (✉) · M. Wang (✉)
Department of Polymer Science and Engineering, State Key Lab of Silicon Materials, Zhejiang University, Hangzhou 310027, P.R. China
e-mail: hzchen@zju.edu.cn

M. Wang
e-mail: mwang@zju.edu.cn

Y.-G. Han · G. Wu · H.-Z. Chen · M. Wang
Key Laboratory of Macromolecule Synthesis and Functionalization (Zhejiang University), Ministry of Education, Hangzhou 310027, P.R. China

Introduction

Detection of ultraviolet (UV) radiation is becoming important in a number of areas such as environmental monitoring, missile warning systems, space research, and high temperature flame detection. The most common detectors currently in use are the photomultiplier and the silicon photodetector [1, 2]. However, they are not solar-blind and require costly filters to attenuate unwanted radiation [3]. Solar-blind UV photodetectors are conventionally implemented with wide-bandgap inorganic semiconductors such as GaNAl and SiC [1, 2, 4]. However, their manufacturing is complicated and expensive, and is not suitable for large-area applications [5].

On the other hand, organic semiconductors applied in organic solar cells and photodiodes have advanced rapidly in recent years [6–8]. Organic semiconductors in general have the advantages of lower fabrication cost, large-area scalability, and variety in substrates, which make them attractive for consumers or portable electronics. Recently, organic UV detectors have been prepared by incorporating organic electron donor with electron acceptor [6, 7]. Composite materials of inorganic semiconductor nanocrystals and conjugated organic molecules have been the topic of great attention due to the possibility of combining the optoelectronic properties of organic molecules with the superior conductivity of inorganic nanoparticles [9].

In this article, organic–inorganic nanostructured hybrids based on *N*,*N*′-diphenyl-*N*,*N*′-bis(3-methylphenyl)-(1,1′-biphenyl)-4,4′-diamine (MTPD, seen in Fig. 1) and anatase TiO_2 were prepared by layer-by-layer deposition method. Photoreceptors based on MTPD/TiO_2 hybrids were prepared, in which photoactive MTPD was applied as the photogenerating and the hole transport material, and TiO_2 as the electron transport material. It is known that MTPD

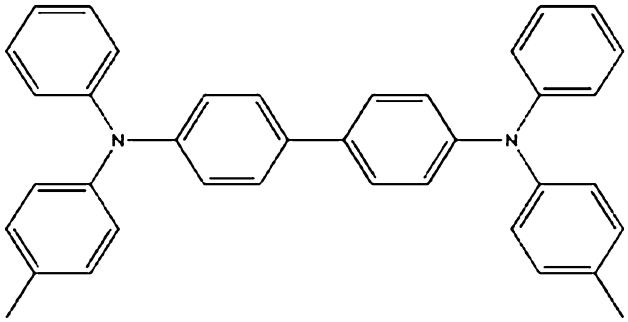

Fig. 1 Molecular structure of *N*,*N*′-diphenyl-*N*,*N*′-bis(3-methylphenyl) -(1,1′-biphenyl)-4,4′-diamine

shows a high hole mobility of about 10^{-2} cm^2 V^{-1} s^{-1} [10]. MTPD also has low optical absorption in the visible region, good energy level matching with TiO_2, and amorphous smooth film morphology [11]. In view of the usage of TiO_2 in solar cells, it is expected that MTPD/TiO_2 hybrid can provide large interface area, thus resulting in high efficiency of charge separation. The obtained MTPD/TiO_2 hybrids photoreceptors might find their applications in UV detection.

Experimental

TiO_2 thin films were prepared by tetrabutyltitanate (TBT), which is generally used for TiO_2 thin films or TiO_2 fine particles by the sol–gel method. TiO_2 colloid solution was prepared as follows: 20 mL of TBT was dispersed in 60 mL of anhydrous ethanol in ambient air. After 30 min of stirring, 16 mL of a mixture of deionized water, acetic acid, and ethanol with a volume ratio of 1:2:5 was dropwise added to the system with agitation. The yellow transparent colloid was obtained 2 h later. Nanoporous TiO_2 films were formed on different substrates through spin-coating the colloid for 15 s. After dried under 80 °C for 30 min, the films were dipped into a dichloromethane solution of MTPD (10% wt/v) and held under 80 °C for half an hour. Figure 2 gives the structure of photoreceptors applied for photoconductivity measurements.

The crystalline structure of TiO_2 powders was investigated by a Rigaku D/max-r X-ray diffractometer using graphite monochromated CuK_α radiation. The morphology of TiO_2 films was examined by scanning electron microscopy (SEM). UV–Vis absorption spectra of TiO_2 and MTPD/TiO_2 films on quartz substrates were obtained on a Varian Cary 100 Bio UV–Vis spectrometer. Photoconductivity was measured using the standard photoinduced discharge method on the GDT-II model photoconductivity measuring device with a 500 W xenon lamp with a filter as a UV light source, and the photosensitivity was expressed as $(E_{1/2})^{-1}$ ($E_{1/2}$= I × $t_{1/2}$, I: light intensity, $t_{1/2}$: time from

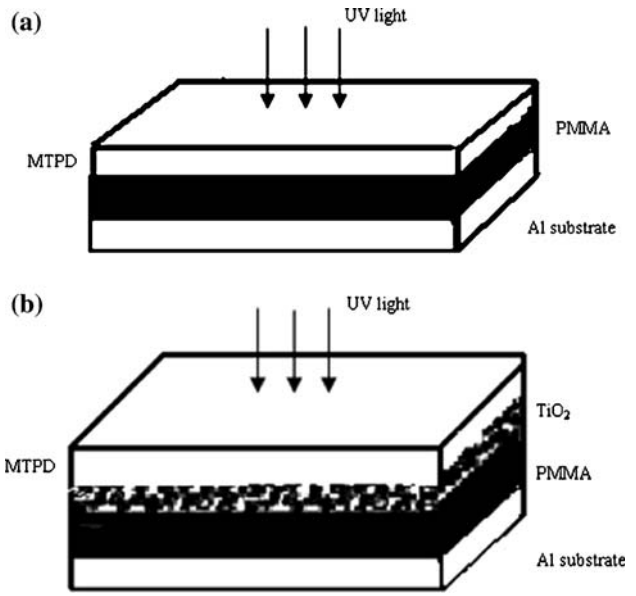

Fig. 2 Schematic diagram of the photoreceptors: (**a**) single layered; (**b**) double layered

the initial potential to half under exposure). The surface photovoltage spectroscopy (SPS) measurements were carried out in an ITO/sample/ITO sandwiched structure as shown in Fig. 3 under the monochromatic light, which was obtained by passing the light from a 500 W xenon lamp through a double-prism monochromator. A lock-in amplifier, synchronized with a light chopper, was employed to amplify the photovoltage signal.

Results and discussion

XRD measurement of TiO_2 powders

Figure 4 gives X-ray diffraction pattern of the TiO_2 nanoparticles synthesized by sol-gel method. The typical peaks owing to the (101), (004), (200), (105) reflections of

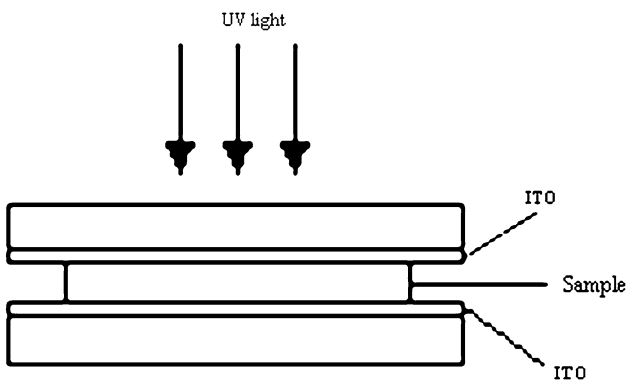

Fig. 3 Schematic representation of the sandwiched structure applied to surface photovoltage spectroscopy measurements

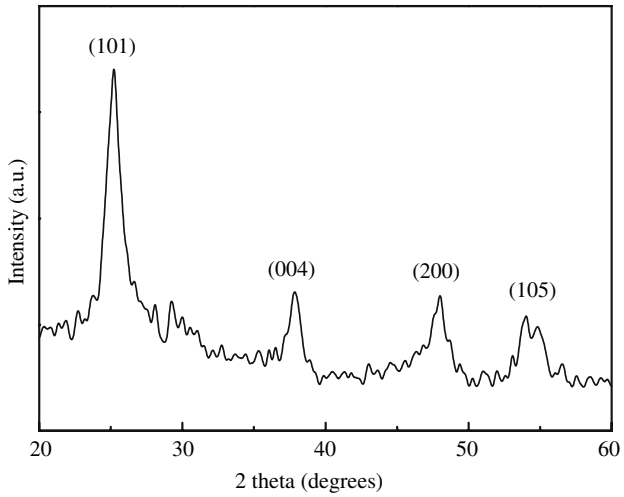

Fig. 4 X-ray diffraction pattern of TiO_2 powders

the anatase phase can be found at $2\theta = 25.3$, 38, 48, and 54° [12]. There are no peaks at 27.5 and 30.8°, which correspond to the (110) and (121) reflections of rutile and brookite [13]. These observations indicate that the obtained TiO_2 nanoparticles are anatase.

Surface morphology of the TiO_2 film

The morphology of TiO_2 film spin-coated on the ITO glass is shown in Fig. 5. It is found that the TiO_2 film presents porous structure, which could greatly enhance the surface area of the film and ease the interpenetration of MTPD into the TiO_2 film. Thus, the area of the interface between TiO_2 and MTPD increased obviously. It is believed that the enlargement of the contact area between TiO_2 and MTPD will facilitate the separation of electron-hole pairs at the interface.

UV–Vis absorption

Figure 6 displays the UV–Vis absorption spectra of MTPD and MTPD/TiO_2 films on the quartz substrates at room temperature. The main absorption band of the films is below 420 nm. Compared with MTPD film, the maximum absorption of MTPD/TiO_2 hybrid film is slightly blue-shifted, which indicates the difference of the aggregated structure between MTPD and MTPD/TiO_2 film. Similar phenomenon was also observed in P3MeT/TiO_2 system [14].

Photoconductivity

Figure 7 presents the photosensitivity of photoreceptors made from TiO_2, MTPD, and MTPD/TiO_2 bilayer composite. It is found that the photoconductivity of the MTPD/TiO_2 composite is higher than that of MTPD, while the photoconductivity of TiO_2 can be ignored compared with that of MTPD because the half-discharge time of TiO_2 is much higher than that of MTPD. That is to say, the

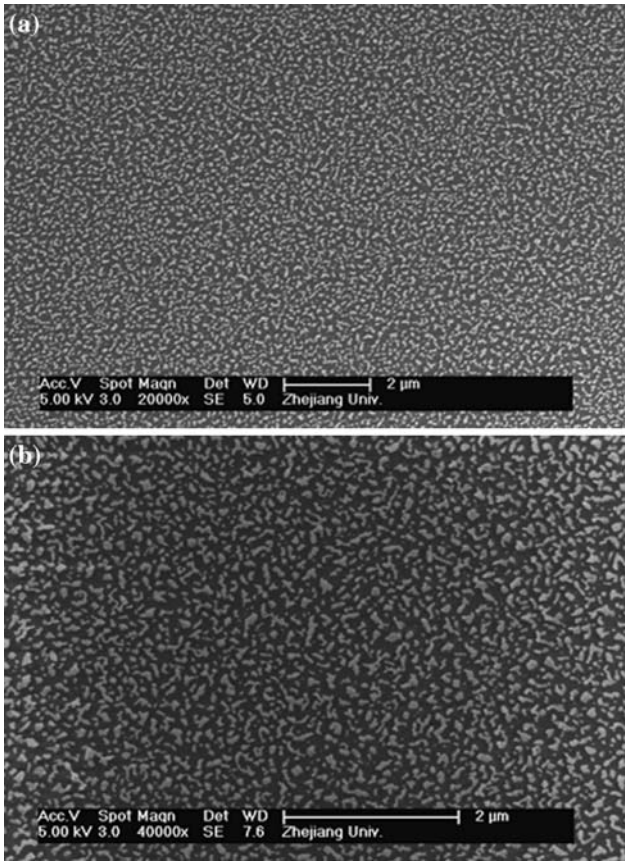

Fig. 5 SEM images of TiO_2 film: (**a**) 20,000 magnitude; (**b**) 40,000 magnitude

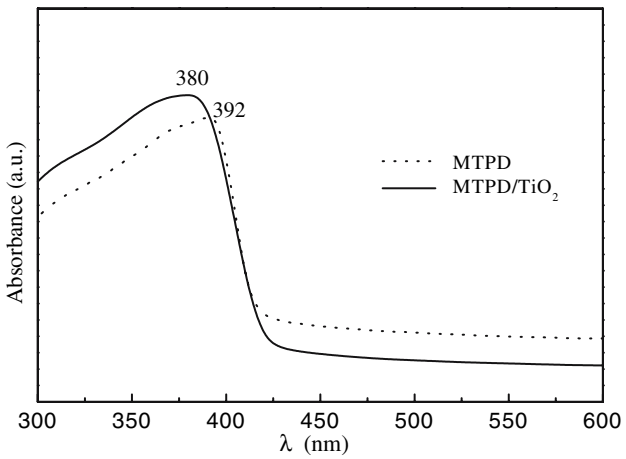

Fig. 6 UV–Vis absorption spectra of MTPD and MTPD/TiO_2 bilayer films

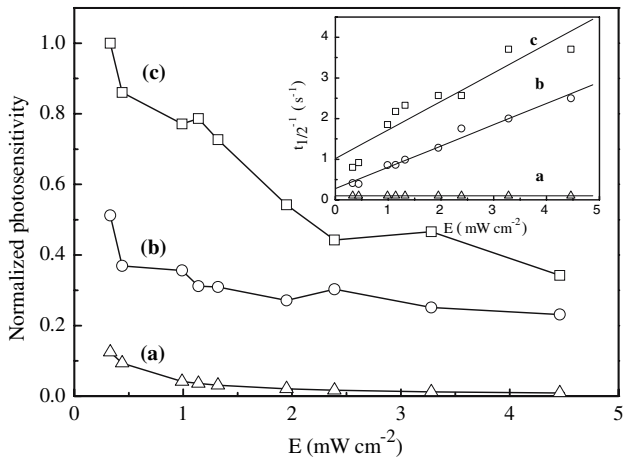

Fig. 7 Photosensitivity of (a) TiO_2, (b) MTPD, and (c) MTPD/TiO_2. Inset: Light intensity dependence of $t_{1/2}^{-1}$ for TiO_2, MTPD, and MTPD/TiO_2

addition of TiO_2 layer helps to improve the photosensitivity of the photoreceptors.

MTPD is a hole transport material with absorption in UV region. A large interface area between MTPD and TiO_2 could be achieved in MTPD/TiO_2 bilayer composite film by dipping TiO_2 nanoporous film into MTPD containing solution. When the photoreceptor was exposed to UV light ranging from 280 to 420 nm, MTPD acted as a charge generation material. The excitons generating in MTPD film moved to the large interface between TiO_2 and MTPD for separation. The free electrons were injected into the conducting band of TiO_2 and diffused/drifted to the anode. The increased photosensitivity of the device was resulted from the efficient separation of excitons due to the large interface between MTPD and TiO_2, and the convenient transport of free charges to the corresponding electrodes. Energy band structure of TiO_2/MTPD bilayer composite was shown in Fig. 8. The LUMO of MTPD is above the bottom of the conduction band of TiO_2, so the electron injection from the organic MTPD to TiO_2 is energetically favorable [15]. Therefore, they can be formed to be a donor/acceptor pair as a photoactive layer.

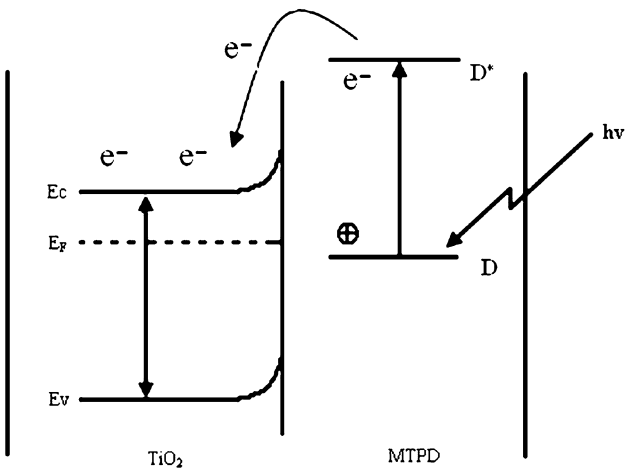

Fig. 8 Energy band structure of TiO_2/MTPD bilayer composite

In general, the enhancement of the light intensity will increase the number of the photoinduced excitons in the materials. Thus, as shown in the inset of Fig. 7, the photoconductive response velocity (in the form of $t_{1/2}^{-1}$) of the photoreceptor increases linearly with the increasing intensity of the incident light. While, as shown in Fig. 7, the photosensitivity expressed by $E_{1/2}$ does not increase with the increasing light intensity. On the contrary, the photosensitivity of the photoreceptors decreases with the intensification of the UV light. Although the enhancement of the UV light increases the amount of photoinduced excitons, not all of these excitons could transport to the electrodes for the reason that many of them are quenched during the transportation. Thus the extent of the net increase of photoinduced excitons cannot match the UV enhancement.

Effects of film thicknesses on the performance of the photoreceptors were also studied. As shown in Fig. 9, the photosensitivity of our bilayer device increases with the decreasing spin rate. It is obvious that the thickness of the TiO_2 film increases with the decreasing spin rate. As the thickness of the films increases, more organic molecules penetrate into the pores of TiO_2, and the contact area between TiO_2 and MTPD was enlarged, which facilitates the separation of the UV-induced excitons.

Since the photoreceptors will be operated under UV illumination, one may concern about the stability of organic materials to UV-induced damage. Figure 10 gives the time dependence of photosensitivity of the unencapsulated MTPD/TiO_2/Al photoreceptor exposed to different UV intensities. It is found that when the illumination

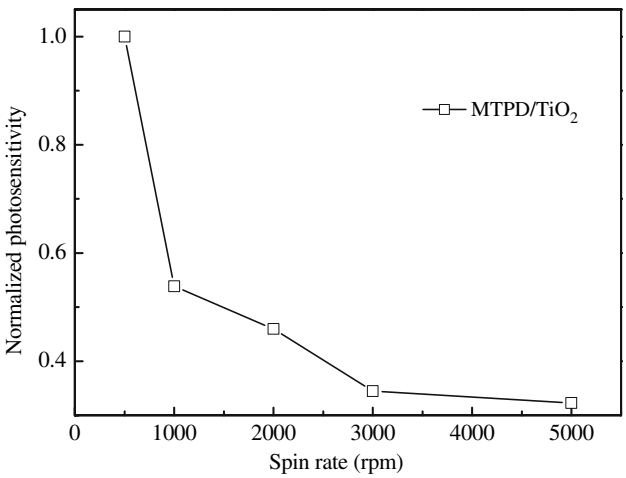

Fig. 9 Effects of the thicknesses of TiO_2 films on photosensitivity under UV illumination of 0.3 mW cm^{-2}

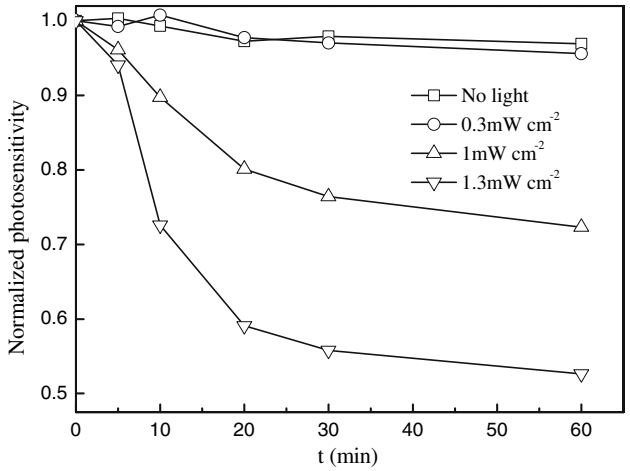

Fig. 10 Stability of photoreceptors exposed to different intensities of UV light

intensity is below 1 mW cm^{-2}, an intensity similar to the total UV portion of the solar spectrum reaching the earth surface [6] and the attenuation of the photosensitivity within 1 h is less than 5% and the variation of the photosensitivity is independent of the UV light, which offers the potential application in the field of UV detection. When UV intensity is beyond 1 mW cm^{-2}, the property of the device deteriorated rapidly due to photooxidation of the organic component of MTPD [16, 17]. Thus more efforts such as developing more stable organic semiconductors and careful device encapsulation should be done to enhance the stability of the device.

Surface photovoltage spectra

The surface photovoltage spectrum (SPS), consisting of the change in the surface potential barrier upon illumination, was applied to investigate the electron processes in the composites [18, 19]. As shown in Fig. 11a and c, the surface photovoltage response of the MTPD/TiO_2 hybrid at about 370 nm is higher compared with that of the pure MTPD, indicating that the dissociation of photoinduced species is more efficient in the MTPD/TiO_2 hybrid due to the photoinduced charge transfer from MTPD to TiO_2. It is suggested that TiO_2 can act as good electron acceptor, and charge transfer is magnified in the TiO_2-based hybrid system. It is thus reasonable to draw the conclusion that there is efficient charge transfer from MTPD to TiO_2.

On the other hand, as shown in Fig. 11b, the surface photovoltage response of TiO_2 film is almost imperceptible compared with that of MTPD. While in Fig. 11d, with the addition of the MTPD layer, the SPS signals appear at 336 and 380 nm, in which the SPS response at 380 nm is related to MTPD molecules infiltrating into the porous TiO_2 film. According to the photocurrent response shown in the inset of Fig. 11, the SPS signal at 336 nm is

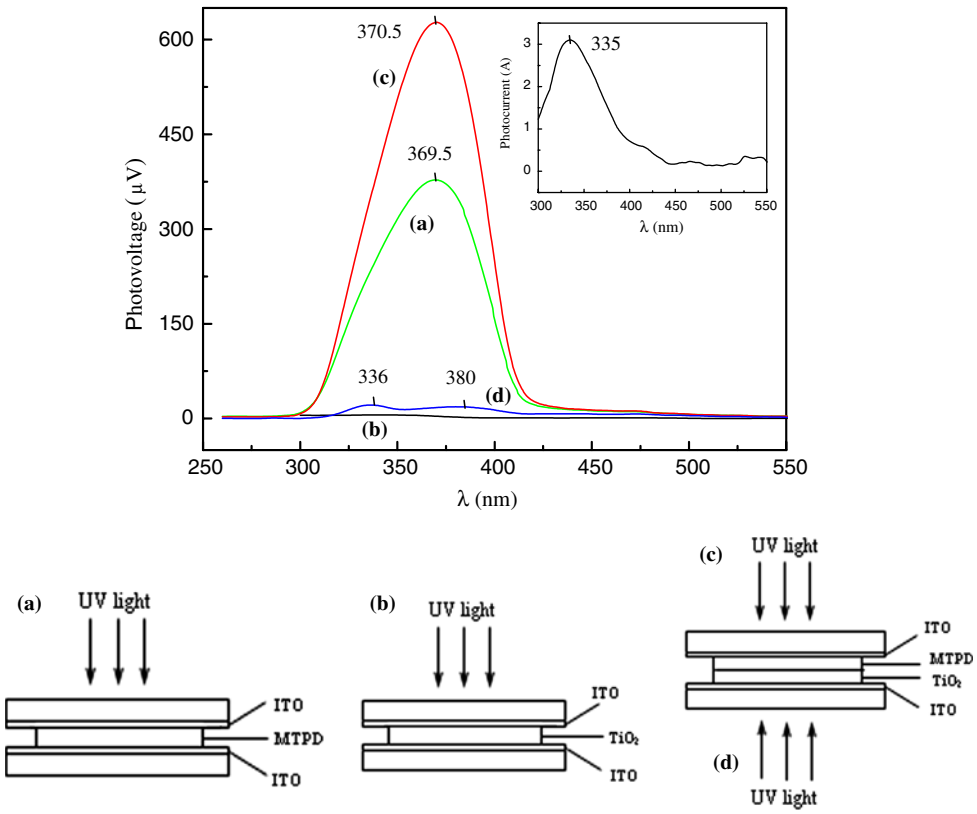

Fig. 11 Surface photovoltage response of (**a**) MTPD, (**b**) TiO_2, and (**c**, **d**) MTPD/TiO_2 bilayer composite. The inset shows the photocurrent of TiO_2 film (external bias 10 V)

correlated with the TiO_2 layer. Upon illumination, excitons created within the TiO_2 layer may diffuse or drift to the space charge region and separate there. That is to say, because of the photoinduced charge transfer from TiO_2 to MTPD, the SPS response at 336 nm of TiO_2/MTPD bilayer film is much more obvious than that of pure TiO_2 film.

Conclusions

In summary, organic–inorganic nanostructured hybrids based on wide-bandgap MTPD and anatase TiO_2 were prepared via layer-by-layer deposition method, in which MTPD acts as electron donor and anatase TiO_2 as electron acceptor. With the increasing intensity of the incident light, the photoconductive response velocity (in the form of $t_{1/2}^{-1}$) of the photoreceptor increases linearly and the photosensitivity expressed by $E_{1/2}$ decreases because of the quenching of the photoinduced excitons during the transportation to the electrodes. The photosensitivity of the bilayer photoreceptor increases with the increasing thickness of the TiO_2 film because of the enlargement of the contact area between TiO_2 and MTPD, which facilitates the separation of the UV-induced excitons. The SPS measurements indicated the existence of the efficient light-induced charge transfer from MTPD to TiO_2, which was responsible for the fact that the UV photosensitivity of the photoreceptor made from MTPD/TiO_2 nanostructured hybrids was two times higher than that of MTPD. The overlap of the spectral response in the UV-A (320–400 nm) range endows them potential applications in UV photodetection.

Acknowledgements This work was supported by National Natural Science Foundation of China (Grant No. 50433020, 50520150165, 50503021, 50773067).

References

1. Razeghi M, Rogalski A (1996) J Appl Phys 79:7433
2. Monroy E, Omnes F, Calle F (2003) Semicond Sci Tech 18:R33
3. Xu Z-Q, Deng H, Xie J, Li Y, Li Y-R (2005) J Sol–Gel Sci Techn 36:223
4. Goldberg YA (1999) Semicond Sci Tech 14:R41
5. Yamaura Y, Muraoka Y, Yamauchi T, Yamauchi T, Muramatsu T, Hiroi Z (2003) Appl Phys Lett 83:2097
6. Lin H-W, Ku S-Y, Su H-C, Huang C-W, Lin Y-T, Wong K-T, Wu C-C (2005) Adv Mater 17:2489
7. Chen L-L, Li W-L, Wei H-Z, Chu B, Li B (2006) Sol Energy Mater Sol Cells 90:1788
8. Tsuzuki T, Shirota Y, Rostalski J, Meissner D (2000) Sol Energy Mater Sol Cells 61:1
9. Zhou X-S, Li Z, Wang N, Lin Y-H, Nan C-W (2006) Appl Phys Lett 88:243119
10. Heun S, Borsenberger PM (1995) Chem Phys 200:245
11. Huang Q-L, Evmenenko GA, Dutta P, Lee P, Armstrong NR, Marks TJ (2005) J Am Chem Soc 127:10227
12. Pomoni K, Vomvas A, Trapalis C (2005) Thin Solid Films 479:160
13. Bhattacharyya A, Kawi S, Ray MB (2004) Catal Today 98:431
14. Lin Y-J, Wang L, Chiu W-Y (2006) Thin Solid Films 511–512:199
15. Ji J-S, Lin Y-J, Lu H-P, Wang L, Rwei S-P (2006) Thin Solid Films 511–512:182
16. Makarov VI, Kochubei SA, Khmelinskii IV (2002) Chem Phys Lett 355:504
17. Sakai N, Prasad GK, Ebina Y, Takada K, Sasaki T (2006) Chem Mater 18:3596
18. Zhang J, Wang D-J, Shi T-S, Wang B-H, Sun J-Z, Li T-J (1996) Thin Solid Films 284–285:596
19. Cao J, Sun J-Z, Hong J, Li H-Y, Chen H-Z, Wang M (2004) Adv Mater 16:84